Trapping analysis of a magnetic electron by a circularly polarized electromagnetic wave in static electric field

Abstract

An pseudo-potential model is presented to illustrate the trapping effect of electrons in a static electric field by an electromagnetic wave through Normal Doppler Resonance (NDR) and Anomalous Doppler Resonance (ADR) under a uniform background magnetic field. When the electromagnetic wave intensity surpasses a threshold, the electron's parallel velocity becomes trapped and oscillates within a pseudo-potential well. In this trapping region, energy from the static electric field is continuously converted into gyrokinetic energy. The energy transfer ratio from the static electric field to the gyrokinetic is calculated and compared with predictions from quantum theory, showing good agreement.

I. Introduction

The manipulation of particles via electromagnetic (E.M) waves is a powerful and versatile technique, primarily employed for two key objectives: particle acceleration and trapping. In the context of acceleration, one prominent mechanism is autoresonance, wherein a charged particle sustains phase synchronization with an E.M wave through nonlinear effects. A well-known example is the Gyro-Resonant Accelerator[1-3], in which electrons resonate within a time-varying magnetic field while interacting with a fixed-frequency E.M wave, the smooth augmentation of the magnetic field is automatically accompanied by a correspondent growth of the relativistic electron mass. Additional acceleration mechanisms include betatron resonance[4-6] and ponderomotive-force-driven acceleration[7, 8]. On the other hand, Velocity-accelerating can also be achieved through Landau resonant, wherein electrons with velocities near the phase velocity of a longitudinal wave become confined within the associated potential well[9], and then through increasing the phase velocity along the electron trajectory, the electron will also be accelerated due to the trapping effect. For particle trapping, spatial confinement can be achieved using methods such as optical tweezers or ponderomotive potential wells generated by the spatial interference patterns of laser beats [10].

Besides the physics application, Ream of papers describe the phenomenon of the trapping effect between E.M wave and electron in universal space and plasma device such as tokamak. For example, the trapped electron in chorus wave nonlinearity or time domain structures (TDS)[11], the relativistic electron precipitation by EMIC waves (electromagnetic ion cyclotron mode[12]), and the resonance with whistle mode wave[13].

Although the interaction between test particles and E.M waves has been extensively studied[14-22], like the resonant between electron and electrostatic field or electromagnetic wave under magnetic field [23, 24].Few studies have incorporated the static electric field into the interactions between electron and E.M wave under magnetic field, despite its relevance in phenomena such as runaway electron generation in tokamaks[25] and pitch angle scattering in earth space[11] [26], where there exist both the electrostatic field, background magnetic field and E.M wave likes whistle wave[11]; Building upon pseudopotential approaches used to study electron pitch-angle scattering in E.M waves[14], we extend existing models by introducing a static electric field, thereby uncovering a previously unexplored form of

resonant trapping in E.M wave–particle interactions. To the best of our knowledge, in this study we first numerically investigate trapping phenomenon in which electron's velocity within a static electric field become confined at the Normal Doppler Resonant or Anomalous Doppler Resonant in a uniform magnetic field. During trapping, the work performed by the static electric field is continuously converted into gyrokinetic energy or E.M wave, thereby sustaining resonance condition with the E.M wave, and the energy transfer from static electric field also agree with the quantum theory prediction and satisfied with angular conservation model[27].

The structure of this paper is as follows: In Section II, we develop a mathematical framework describing the interaction between an electromagnetic wave and an electron subjected to a static electric field that is colinear with a uniform background magnetic field. Section III presents a numerical investigation of the resulting trapping dynamics, including a detailed analysis of the underlying physical mechanism and the derivation of critical threshold conditions necessary for trapping. In Section IV, the theoretical predictions are benchmarked against results from quantum theory to assess consistency and validate the model. Section V offers a comprehensive discussion of the findings, and Section VI concludes the paper with a summary of the principal results and their potential implications.

II. electron-electromagnetic wave interaction analysis

2.1 Field equations

To analyze interaction between electron and E.M wave, we consider an E.M wave propagate along uniform magnetic field whose phase velocity $\mathrm{v_T} = \omega/\mathrm{k}$, where ω is the angular frequency and k is the wavenumber. The uniform background magnetic field is $B_o = B_o\hat{z}$. The wave's magnetic field perturbation $\tilde{B}$ is characterized by the dimensionless parameter $\kappa \equiv |\tilde{B}|/B_o$, such that the total magnetic field becomes $\mathbf{B} = B_o\hat{z} + \tilde{B}$. The system includes a static electric field $E_o = E_o\hat{z}$, with the total electric field given by $\mathbf{E} = E_o\hat{z} + \tilde{E}$, where $\tilde{E}$ represents the electric field components of E.M wave:

$$\tilde{\mathbf{E}} = \mathrm{E_w}\,[\hat{\mathrm{x}}\cos(\mathrm{kz} - \omega\mathrm{t}) + g\,\hat{\mathrm{y}}\sin(\mathrm{kz} - \omega\mathrm{t})] \tag{1}$$

Here, $\mathrm{E_w}$ is the electric field amplitude of E.M wave, and the polarization satisfies the left-hand circular polarization (LCP) condition when g = 1, and right-hand circular polarization (RCP) condition when g = -1.

Faraday's law requires the associated magnetic field to be

$$\widetilde{\boldsymbol{B}} = \frac{k}{\omega}\hat{z} \times \widetilde{\boldsymbol{E}} = \kappa B_0[-g\,\hat{x}\sin(kz - \omega t) + \hat{y}\cos(kz - \omega t)] \tag{2}$$

Here $\kappa B_0 = \mathrm{B_w} = \frac{\mathrm{k}}{\omega}E_w$.

2.2 Transformation to the wave frame

In wave frame, which denotes as prime and moves at constant velocity $\mathrm{v_T} = \omega/\mathrm{k}$ with respect to the lab frame, the fields are

$$E'_{\parallel} = E_{\parallel} \tag{3}$$

$$B'_{\parallel} = B_{\parallel} \tag{4}$$

$$E'_{\perp} = \gamma_T(\boldsymbol{E} + v_T \times \boldsymbol{B})_{\perp} \tag{5}$$

$$B'_{\perp} = \gamma_T \left(\boldsymbol{B} - \frac{1}{c^2} v_T \times \boldsymbol{E} \right)_{\perp} \tag{6}$$

Where $\gamma_T = 1/\sqrt{1 - \left(\frac{v_T}{c}\right)^2}$. Substituting the wave fields Eq. (1), Eq. (2) into Eq.(5), Eq. (6) gives $E'_{\perp} = 0$ and $B'_{\perp} = \frac{B_{\perp}}{\gamma_T}$.

Since $\{\boldsymbol{k}, \frac{i\omega}{c}\}$ and {**x**, ict} are relativistic four-vectors, we have

$$kz - \omega t = k\gamma_T(z' + v_T t') - \omega\gamma_T \left(t' + \frac{v_T z'}{c^2} \right) = k'z' \tag{7}$$

Here $k' = k/\gamma_T$ and z′ are the wavenumber and position in the wave frame. The magnetic field of E.M wave is

$$\boldsymbol{B}'_{\perp} = B'_{\perp}(-g\, \hat{x} \sin(k'z') + \hat{y} \cos(k'z') \tag{8}$$

The motion equation of the charge particle in the prime frame is

$$\frac{d}{dt'}(\gamma'\beta') = \frac{q}{m}\left(\frac{E_0}{c} \hat{z} + \beta' \times B' \right) \tag{9}$$

Where $\gamma' = 1/\sqrt{1 - \beta'^2}$, m is the rest mass of electron and q is the electron charge with q = -e. Note that γ,γ_T, and γ' differ and should not be confused with each other. The derivation of energy γ′ to t' and the motion equation in each direction should be

$$\frac{d\gamma'}{dt'} = \frac{qE_0 \hat{z} \cdot \beta'_z}{mc} \tag{10}$$

$$\frac{d}{dt'}(\gamma'\beta'_z) = \Omega \left(\frac{E_0}{cB_0} \hat{z} + \beta'_{\perp} \times \frac{B'_{\perp}}{B_0} \right) \tag{11}$$

$$\frac{d}{dt'}(\gamma'\beta'_{\perp}) = \Omega \left(\beta'_{\perp} \times \hat{z} + \beta'_z \hat{z} \times \frac{B'_{\perp}}{B_0} \right) \tag{12}$$

Here Ω is the nonrelativistic electron cyclotron frequency in the lab frame with $\Omega < 0$. Introduce

$$\xi_z = 1 + \alpha\gamma'\beta'_z \tag{13}$$

Here $\alpha = \frac{g\omega}{\Omega\gamma_T} n$. And

$$\xi_{\perp} = 1 + \alpha\gamma'\beta'_{\perp} \tag{14}$$

where $n = ck/\omega$, according to Eq. (11) , Eq. (12), we have

$$\frac{d\xi_z}{dt'} = \alpha\Omega \left(\frac{E_0}{cB_0} \hat{z} + \frac{\xi_{\perp} - 1}{\alpha\gamma'} \times \frac{B'_{\perp}}{B_0} \right) \cdot \hat{z} \tag{15}$$

$$\frac{d\xi_{\perp}}{dt'} = \alpha\Omega \left(\frac{\xi_{\perp} - 1}{\alpha\gamma'} \times \hat{z} + \frac{\xi_z - 1}{\alpha\gamma'} \hat{z} \times \frac{B'_{\perp}}{B_0} \right) \tag{16}$$

2.3 Construction of pseudo-potential problem

Taking the derivative of Eq. (15) with respect to t' gives

$$\frac{d^2\xi_z}{dt'^2} = \alpha\Omega\left(\frac{d}{dt'}\left(\frac{\xi_\perp - 1}{\alpha\gamma'}\right)\times\frac{B'_\perp}{B_0}\right)\cdot\hat{z} + \alpha\Omega\left(\frac{\xi_\perp - 1}{\alpha\gamma'}\times\frac{d}{dt'}\left(\frac{\boldsymbol{B}'_\perp}{B_0}\right)\right)\cdot\hat{z} \tag{17}$$

And

$$\frac{d}{dt'}\left(\frac{\xi_\perp - 1}{\alpha\gamma'}\right) = \frac{1}{\alpha\gamma'}\cdot\frac{d\xi_\perp}{dt'} - \frac{\xi_\perp - 1}{\alpha\gamma'^2}\frac{d\gamma'}{dt} \tag{18}$$

According to Eq. (10) and ξ_z, we have

$$\frac{d\gamma'}{dt} = \Omega\frac{E_0}{B_0 c}\frac{\xi_z - 1}{\alpha\gamma'} \tag{19}$$

While in Eq. (16), consider typically $\beta'_\perp \ll \beta'_z$ and $B'_\perp < B_0$ which is suitable in most case of Tokamak environment, we have

$$\frac{d\xi_\perp}{dt'} < \Omega\frac{\xi_z - 1}{\gamma'} \tag{20}$$

Finally, in the right side of Eq. (18)

$$\frac{\left|\frac{\xi_\perp - 1}{\alpha\gamma'^2}\cdot\frac{d\gamma'}{dt}\right|}{\left|\frac{1}{\alpha\gamma'}\cdot\frac{d\xi_\perp}{dt'}\right|} < \frac{E_0\beta'_\perp}{B_0 c} \tag{21}$$

While for $\beta'_\perp \ll 1$ and $\frac{E_0}{B_0 c} \ll 1$, which is satisfied in most of situation, we can confidently ignore the second term in the right side of Eq. (18), then

$$\frac{d}{dt'}\left(\frac{\xi_\perp - 1}{\alpha\gamma'}\right) = \frac{1}{\alpha\gamma'}\cdot\frac{d\xi_\perp}{dt'} \tag{22}$$

Combing Eq. (17) with Eq. (22), we have

$$\frac{d^2\xi_z}{dt'^2} = \alpha\Omega\left(\frac{1}{\alpha\gamma'}\cdot\frac{d\xi_\perp}{dt'}\times\frac{B'_\perp}{B_0}\right)\cdot\hat{z} + \alpha\Omega\left(\frac{\xi_\perp - 1}{\alpha\gamma'}\times\frac{d}{dt'}\left(\frac{\boldsymbol{B}'_\perp}{B_0}\right)\right)\cdot\hat{z} \tag{23}$$

Substituting Eq. (16) into Eq. (23) gives

$$\frac{d^2\xi_z}{dt'^2} = \alpha\Omega\left[\frac{\Omega}{\gamma'}\left(\beta'_\perp\times\hat{z} + \beta'_z\hat{z}\times\frac{B'_\perp}{B_0}\right)\times\frac{B'_\perp}{B_0} + \beta'_\perp\times\frac{d}{dt'}\left(\frac{\boldsymbol{B}'_\perp}{B_0}\right)\right]\cdot\hat{z} \tag{24}$$

The time derivation of wave magnetic field in wave frame is

$$\frac{d\boldsymbol{B}'_\perp}{dt'} = -k'\frac{dz'}{dt'}B'_\perp(g\,\hat{x}\cos(k'z') + \hat{y}\sin(k'z') = g\omega n'\beta'_z\hat{z}\times\boldsymbol{B}'_\perp \tag{25}$$

where $n' = \frac{ck'}{\omega} = n/\gamma_T$. By substituting Eq. (25) into Eq. (23) and simplify Eq. (23) gives

$$\frac{d^2\xi_z}{dt'^2} = \frac{\alpha\Omega^2}{\gamma'}\left(\frac{\beta'_\perp \cdot \boldsymbol{B}'_\perp}{B_0}(1 + \frac{g\omega n}{\Omega\gamma_T}\gamma'\beta'_z) - \beta'_z\frac{\boldsymbol{B}'_\perp}{B_0}\cdot\frac{\boldsymbol{B}'_\perp}{B_0}\right) \tag{26}$$

Since $\xi_z = 1 + \frac{g\omega n}{\Omega\gamma_T}\gamma'\beta'_z$, finally

$$\frac{d^2\xi_z}{dt'^2} = \frac{\alpha\Omega^2}{\gamma'}\left(\frac{\beta'_\perp \cdot \boldsymbol{B}'_\perp}{B_0}\xi_z - \beta'_z\frac{\boldsymbol{B}'_\perp}{B_0}\cdot\frac{\boldsymbol{B}'_\perp}{B_0}\right) \tag{27}$$

2.3.1 connect $\frac{\boldsymbol{\beta}'_\perp\cdot\boldsymbol{B}'_\perp}{\boldsymbol{B_0}}$ with ξ_z

To obtain the relationship between $\frac{\boldsymbol{\beta}'_\perp\cdot\boldsymbol{B}'_\perp}{\boldsymbol{B_0}}$ and ξ_z, taking the time derivation of $\frac{\beta'_\perp\cdot\boldsymbol{B}'_\perp}{B_0}$ gives

$$\frac{\mathrm{d}}{\mathrm{d}t'}\left(\frac{\beta'_\perp \cdot \boldsymbol{B}'_\perp}{B_0}\right) = \frac{d\beta'_\perp}{dt'}\cdot\frac{\mathrm{B}'_\perp}{B_0} + \beta'_\perp\cdot\frac{d}{dt'}\left(\frac{\mathrm{B}'_\perp}{B_0}\right) \tag{28}$$

where

$$\frac{d\beta'_\perp}{dt'}\cdot\frac{\mathrm{B}'_\perp}{B_0} = -\hat{z}\cdot\left(\beta'_\perp\times\frac{B'_\perp}{B_0}\right)\Omega' - \Omega'\frac{E_0\beta'_z}{cB_0}\left(\beta'_\perp\cdot\frac{B'_\perp}{B_0}\right) \tag{29}$$

and

$$\beta'_\perp\cdot\frac{d}{dt'}\left(\frac{\mathrm{B}'_\perp}{B_0}\right) = \beta'_\perp\cdot g\omega n'\beta'_z\left(\hat{z}\times\frac{\boldsymbol{B}'_\perp}{B_0}\right) = -g\omega n'\beta'_z\left(\beta'_\perp\times\frac{\boldsymbol{B}'_\perp}{B_0}\right)\cdot\hat{z} \tag{30}$$

Here we ignore the time derivation of γ' in Eq. (12) and $\Omega' = \Omega/\lambda'$. Finally, we have

$$\frac{\mathrm{d}}{\mathrm{d}t'}\left(\frac{\beta'_\perp \cdot \boldsymbol{B}'_\perp}{B_0}\right) = -\xi_z\Omega'\hat{z}\cdot\left(\beta'_\perp\times\frac{B'_\perp}{B_0}\right) - \Omega'\frac{E_0\beta'_z}{cB_0}\left(\beta'_\perp\cdot\frac{B'_\perp}{B_0}\right) \tag{31}$$

The equation is first-order linear differential equation with the form:

$$\mathrm{z}'(\tau) + \mathrm{Pz}(\tau) = \mathrm{Q}(\tau) \tag{32}$$

Where $P = \Omega'\frac{E_0\beta'_z}{cB_0}$, $Q = -\xi_z\Omega'\hat{z}\cdot\left(\beta'_\perp\times\frac{B'_\perp}{B_0}\right)$ and $z = \frac{\beta'_\perp\cdot\boldsymbol{B}'_\perp}{B_0}$. The exact solution of z is

$$\mathrm{z} = \mathrm{e}^{-\int \mathrm{P}\mathrm{d}\tau} * \left[\int e^{\int P d\tau'} Q d\tau + C_0\right] \tag{33}$$

here $\mathrm{P} = \frac{E_0\beta'_z}{cB_0}$ and $\mathrm{Q} = -\xi\hat{z}\cdot\left(\beta'_\perp\times\frac{B'_\perp}{B_0}\right)$, $\tau = \mathrm{t}'\Omega'$. Since P<< 1 in most case, we have

$$\mathrm{z} = \int Q d\tau \tag{34}$$

Here we choose the initial condition $|\beta'_{\perp_0}| \ll 1$, which implies $C_0 = 0$. As a result, the expression Eq. (31) can simplify to:

$$\frac{\mathrm{d}}{\mathrm{d}t'}\left(\frac{\beta'_\perp \cdot \boldsymbol{B}'_\perp}{B_0}\right) = -\xi_z\Omega'\hat{z}\cdot\left(\beta'_\perp\times\frac{B'_\perp}{B_0}\right) \tag{35}$$

The substitution of Eq. (15) into Eq. (35) gives

$$\frac{\mathrm{d}}{\mathrm{dt}'}\left(\frac{\beta_{\perp}' \cdot \boldsymbol{B}_{\perp}'}{B_0}\right) = -\xi_{\mathrm{z}}\Omega'\left(\frac{1}{\alpha\Omega}\frac{d\xi_z}{dt'} - \frac{E_0}{cB_0}\right) \tag{36}$$

Integrating Eq. (36) with t′ gives:

$$\frac{\beta_{\perp}' \cdot \boldsymbol{B}_{\perp}'}{B_0} = -\frac{\xi_z^2 - {\xi_{z_0}}^2}{2\alpha\gamma'} + \frac{E_0}{cB_0}\int \xi_{\mathrm{z}}\Omega' dt' + \frac{\beta_{\perp 0}' \cdot \boldsymbol{B}_{\perp \boldsymbol{0}}'}{B_0} \tag{37}$$

Here ξ_{z0}, $\beta_{\perp 0}'$ and $\boldsymbol{B}_{\perp \boldsymbol{0}}'$ represent the initial condition of ξ_z, $\beta_{\perp}'$ and $\boldsymbol{B}_{\perp}'$.

Noting that t = 0 corresponds to z'=0, since z = 0 at t= 0, and recalling the four vectors {γβ, γ}, we have the relation:

$$\gamma_0'\beta_{\perp 0}' = \gamma_0\beta_{\perp 0} \tag{38}$$

Since $\mathrm{B}_{\perp 0}'$ is in the y direction when z' = 0 as shown in Eq. (8), it follows that

$$\frac{\beta_{\perp 0}' \cdot \boldsymbol{B}_{\perp \boldsymbol{0}}'}{B_0} = \frac{\beta_{y0}' B_{\perp}'}{B_0} = \frac{\gamma_0}{\gamma_0'}\kappa'\beta_{\perp 0}\sin\phi_0 \tag{39}$$

Where ϕ_0 is defined by $\beta_{\mathrm{x0}} = \beta_{\perp 0} cos\phi_0$ and $\beta_{\mathrm{y0}} = \beta_{\perp 0}\sin\phi_0$, $\kappa' = \frac{\kappa}{\gamma_T} = \frac{B_{\perp}'}{B_0}$. With these definitions, Eq. (37) becomes

$$\frac{\beta_{\perp}' \cdot \boldsymbol{B}_{\perp}'}{B_0} = -\frac{\xi_z^2 - {\xi_{z_0}}^2}{2\alpha\gamma'} + \frac{E_0}{cB_0}\int \xi_{\mathrm{z}}\Omega' dt' + \frac{\gamma_0}{\gamma_0'}\kappa'\beta_{\perp 0}\sin\phi_0 \tag{40}$$

The substitution of Eq. (40) into Eq. (27) gives:

$$\frac{d^2\xi_{\mathrm{z}}}{dt'^2} = \frac{\alpha\Omega^2}{\gamma'}\left(\left(-\frac{\xi_z^2 - \xi_{z0}^2}{2\alpha\gamma'} + \frac{E_0}{cB_0}\int \xi_{\mathrm{z}}\Omega' dt' + \frac{\gamma_0}{\gamma_0'}\kappa'\beta_{\perp 0}\sin\phi_0\right)\xi_{\mathrm{z}} - \beta_z'\kappa'^2\right) \tag{41}$$

Simplifying Eq. (41) and substituting ξ_{z} for β_{z}' gives:

$$\frac{d^2\xi_z}{dt'^2} = \Omega'^2\left(\xi_z\left(-\frac{\xi_z^2 - \xi_{z0}^2}{2} + \frac{\varsigma E_0}{cB_0}\int \Omega'\xi_{\mathrm{z}} dt' + \alpha\gamma_0\kappa'\beta_{\perp 0}\sin\phi_0\right) - (\xi_z - 1)\kappa'^2\right) \tag{42}$$

Here

$$\varsigma = g\frac{\omega n}{\Omega\gamma_T}\gamma' \tag{43}$$

Normalization of time t′ with $\tau = \mathrm{t}'\Omega'$ we have

$$\frac{d^2\xi_z}{d\tau^2} = \left(\xi_z\left(-\frac{\xi_z^2 - \xi_{z0}^2}{2} + \frac{\varsigma E_0}{cB_0}\int \xi_{\mathrm{z}} d\tau + \alpha\gamma_0\kappa'\beta_{\perp 0}\sin\phi_0\right) - (\xi_z - 1)\kappa'^2\right) \tag{44}$$

The Eq. (44)could also be written as

$$\frac{d^2\xi_z}{d\tau^2} = -\frac{\partial\psi}{\partial\xi_z} \tag{45}$$

Where

$$-\frac{\partial\psi}{\partial\xi_z}=\left(\xi_z\left(-\frac{\xi_z^2-\xi_{z0}^2}{2}+\frac{\varsigma E_0}{cB_0}\int\xi_z d\tau+\alpha\gamma_0\kappa'\beta_{\perp0}\sin\phi_0\right)-(\xi_z-1)\kappa'^2\right) \tag{46}$$

Multiplying Eq. (45) by $\mathrm{d}\xi_z/\mathrm{d}\tau$ and integrating gives a pseudo-energy equation

$$\frac{1}{2}\left(\frac{d\xi_z}{d\tau}\right)^2+\psi(\xi_z)=W_0 \tag{47}$$

Where

$$\psi=\frac{1}{8}\xi_z^4+\left(\kappa'^2-\frac{\xi_{z0}^2}{2}-gs\kappa' sin\phi_0\right)\frac{\xi_z^2}{2}-\kappa'^2\xi_z-\int\xi_z\frac{\varsigma E_0}{cB_0}\int\xi_z d\tau d\xi \tag{48}$$

And

$$\mathrm{W}_0=\frac{1}{2}\left(\frac{d\xi_z}{d\tau}\right)^2|_{\tau=0}+\psi(\xi_{z0}) \tag{49}$$

Here $s=\frac{\omega n\beta_{\perp0}\gamma_0}{\Omega\gamma_T}$.The pseudo potential ψ can only be solved numerically, as it does not have a regular form involving only the parameter ξ, here ψ also depends on t', which is related to β_z' and $\beta_\perp'$.

2.4 Initial condition

From Eq. (15), we see that

$$\frac{d\xi_z}{d\tau}=g\left(\frac{\omega n}{\Omega\gamma_T}\kappa'\gamma\left(\beta_x\cos(kz-\omega t)+g\beta_y\sin(kz-\omega t)\right)\right)+\frac{\varsigma E_0}{cB_0} \tag{50}$$

Here, we use the relation $\gamma\beta_\perp=\gamma'\beta_\perp'$ and $\kappa'=\mathrm{B}_\perp'/B_0$. At the initial time t = 0 and position z = 0, we have

$$\frac{d\xi_z}{d\tau}|_{\tau=0}=gs\kappa' cos\phi_0+\frac{\varsigma E_0}{cB_0} \tag{51}$$

Where $s=\frac{\omega n\beta_{\perp0}\gamma_0}{\Omega\gamma_T}$

2.6 Solve $\boldsymbol{\beta_\perp}$

According to Eq.(12), multiplying $\gamma'\beta_\perp'$ on both sides gives

$$\frac{1}{2}\frac{d(\gamma'\beta_\perp')^2}{dt'}=\Omega\gamma'\beta_\perp'\cdot\left(\beta_z'\times\frac{B_\perp'}{B_0}\right) \tag{52}$$

Reorganize the equation, we have

$$\frac{1}{2}\frac{d(\gamma'\beta_\perp')^2}{dt'}=-\Omega\gamma'\beta_z'\cdot\left(\beta_\perp'\times\frac{B_\perp'}{B_0}\right) \tag{53}$$

According to Eq.(11), multiplying $\gamma'\beta_z'$ on both sides gives

$$\frac{1}{2}\frac{d(\gamma'\beta_z')^2}{dt'} = \Omega\gamma'\beta_z' \cdot \left(\frac{E_0}{cB_0}\hat{z} + \beta_\perp' \times \frac{B_\perp'}{B_0}\right) \tag{54}$$

Add Eq. (53) and Eq. (54), we have

$$\frac{1}{2}\frac{d(\gamma'\beta_\perp')^2}{dt'} + \frac{1}{2}\frac{d(\gamma'\beta_z')^2}{dt'} = \frac{\Omega\gamma' E_0\beta_z'}{cB_0} \tag{55}$$

Which means energy change ratio equal to work done by static electric field in moving frame.

Using the normalized time $\tau = t'\Omega'$, we have

$$\frac{1}{2}\frac{d(\gamma'\beta_\perp')^2}{d\tau} + \frac{1}{2}\frac{d(\gamma'\beta_z')^2}{d\tau} = \frac{\gamma'^2 E_0\beta_z'}{cB_0} \tag{56}$$

Considering that γ' is mainly determined by β_z', integrating both side with t' gives

$$\beta'^2_\perp = \frac{2}{\gamma'^2|_t} \cdot \int_0^t \frac{\gamma'^2 E_0\beta_z'}{cB_0} d\tau + \left(\beta_{z0}'^2 + \beta_{\perp 0}'^2\right) - \beta'^2_z \tag{57}$$

III. Numerical study of the trapping effect

According to Eq. (45), Eq. (46) and Eq.(51), the velocity β_z' could be numerically solved by ode45, and $\beta_\perp'$ can be determined from Eq.(57). Then, using the four-vector $\{\gamma\beta, \gamma\}$, we have:

$$\gamma = \beta_T\gamma_T\gamma'\beta_z' + \gamma_T\gamma' \tag{58}$$

$$\beta_\perp = \frac{\gamma'\beta_\perp'}{\gamma} \tag{59}$$

$$\beta_z = \frac{\gamma_T\gamma'}{\gamma}(\beta_z' + \beta_T) \tag{60}$$

Finally, all the velocities in lab frame can be solved numerically

3.1 Trapping in anomalous doppler resonance (g = 1)

Quantum analysis indicates that, for anomalous Doppler resonance with electrons, the wave polarization is primarily dictated by the LCP component[27], whereas normal Doppler resonance corresponds to the RCP component. We begin by considering two cases in which a LCP electromagnetic wave interacts with electrons in the presence of a uniform magnetic field and a static electric field.

In case I, considering a scenario where the uniform magnetic field B_0 = 2 T and the static electric field E_0 = −0.2 V/m, both along the z-axis, which are close to typical Tokamak plasma conditions. A plane LCP E.M wave is assumed to propagate along z direction with refractive index $n = 4$ and $\omega = 1.1\ \Omega$. The electric field of E.M wave is set to $E_\omega = 20\ V/m$. The numerical results are shown in Figure 1, For the static electric field $E_0 < 0$, the direction of the electric field is opposite to that of the background magnetic field. As a result, the parallel velocity increases over time, as shown in Figure.1(a). Since here $\alpha < 0$, which is given in Eq.(15), the value of ξ_z decreases as β_z increase according to Eq.(15). When

the parallel velocity satisfies the anomalous doppler resonance condition where $\xi_z = 0$, the perpendicular velocity $\beta_\perp$ increase abruptly, as shown in Figure.1 (b-d), After the parallel velocity exceeds the resonance condition, the $\beta_\perp$ will no longer increase. The phase evolution of ξ_z and $\frac{1}{\Omega'}\frac{d\xi_z}{dt'}$ is shown in fig.(e). It can be observed that the fluctuation of $\frac{1}{\Omega'}\frac{d\xi_z}{dt'}$ is stronger for $\xi_z < 0$ than for $\xi_z > 0$. This is because the change of $\frac{1}{\Omega'}\frac{d\xi_z}{dt'}$ is proportional to $\beta_\perp$ as shown in Eq. (50). Fig 1.(f) illustrates the pseudo-potential $\Delta\psi(\xi)$, defined as $\Delta\psi(\xi) = \psi(\xi) - \psi(\xi_0)$ .The initial pseudo-kinetic energy $W_0 = \frac{1}{2}\left(\frac{d\xi_z}{dt'}\right)^2|_{t'=0}$, which is indicated as red dash line in Fig.1 (f). Although the pseudo-potential increases after the resonance point (ξ<0), the initial pseudo-kinetic energy remains greater than the pseudo-potential throughout, indicating that no trapping occurs.

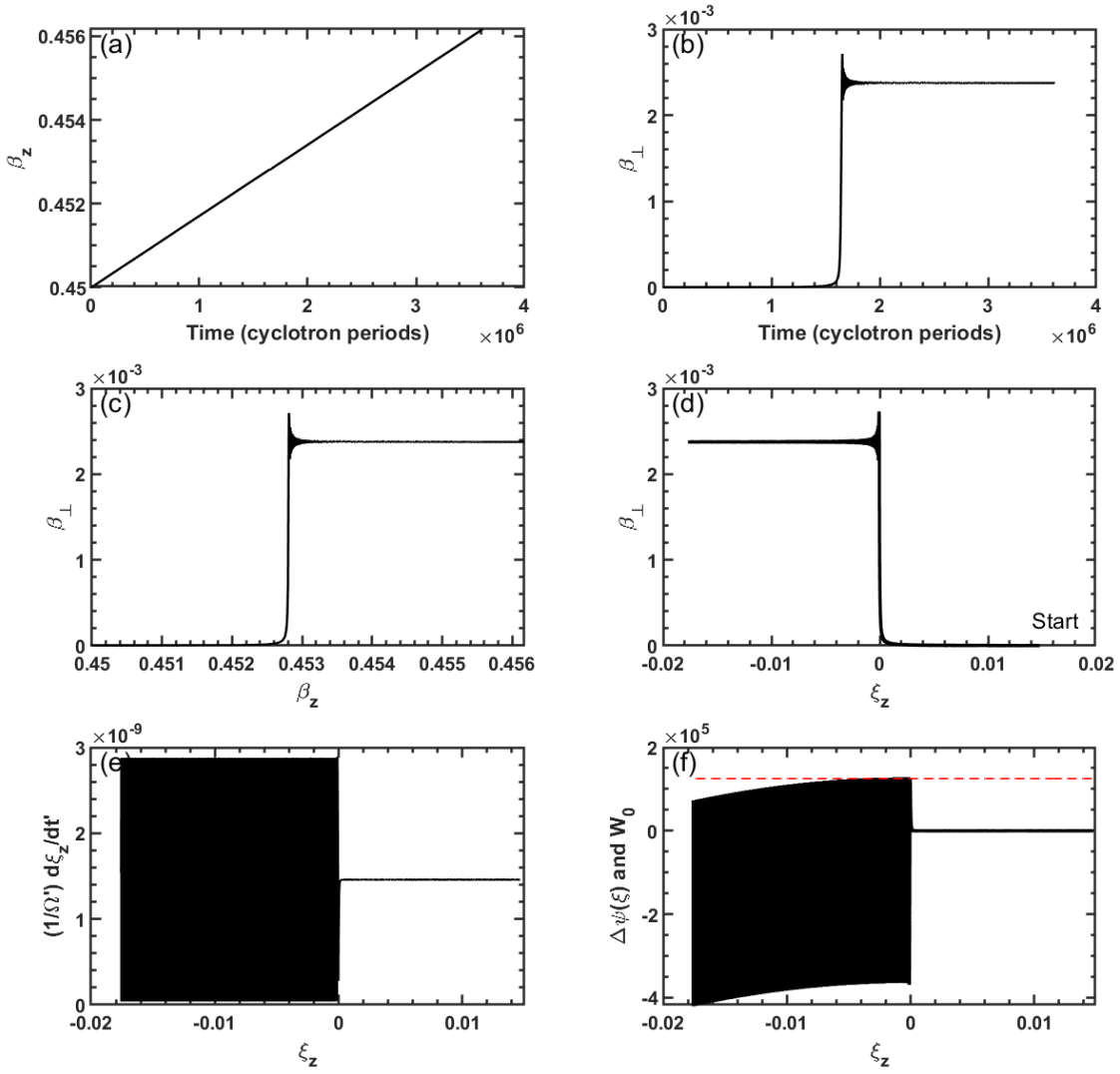

Figure 1. Numerical integration of Eq. (44) *with initial equation Eq.*(51)*. Input parameters are* E_0*=- 0.2 V/m,* E_w *= 20 V/m,* B_0 *= 2 T,* $\omega/\Omega = -1.1$ *,g = 1, initial* β_z*= 0.45 and* $\beta_\perp = 0$*,* $\phi_0 = 0$*, n = 4. This give* $\kappa' \approx 1.29 \times 10^{-7}, \gamma_T = 1.0308, \alpha = -4.373, \gamma_0 = 1.1198$ *and* $\gamma' = 1.0264, \frac{\zeta E_0}{cB_0} = 1.458 \times 10^{-9}$*. (a) The time evolution of* β_z*. (b) The time evolution of* $\beta_\perp$*.(c)The*

velocity phase in (β_z , $\beta_\perp$). (d)The evolution of $\beta_\perp$ with ξ_z. (e) The evolution of $d\xi_z/d\tau$ with ξ_z. (f)The pseudo-potential $\Delta\psi(\xi)$ (black line) and the initial pseudo-kinetic energy E_0 (red dash line)

In case II, the electric field of the LCP E.M wave is increased to 40 V/m. As the electron's parallel velocity approaches the resonant velocity, it no longer increases continuously but begins to oscillate around the resonant velocity, as shown in Fig. 2(a). While on the other hand, the perpendicular velocity increases continuously when β_z trapping in resonant region, as shown in Fig.2 (b-d). The phase trajectory of (ξ_z, $\frac{1}{\Omega'}\frac{d\xi_z}{dt'}$) is shown in Fig.2 (e). The closed-loop structure indicates periodic motion around the resonant point, and the direction of motion is labeled with arrow. The electron can only propagate within the region where the pseudo-potential $\Delta\psi(\xi)$ is lower than the initial pseudo-kinetic energy W_0. When the pseudo-potential tends to surpass the W_0, the electron velocity rebounds upon reaching the boundary of the pseudo-potential well. Consequently, the electron becomes confined within the well, the width of the pseudo-potential well also increases, since it is influenced by the parameter $\beta_\perp$. This bounce effect, shown in Fig.2 (f), illustrates the trapping phenomenon.

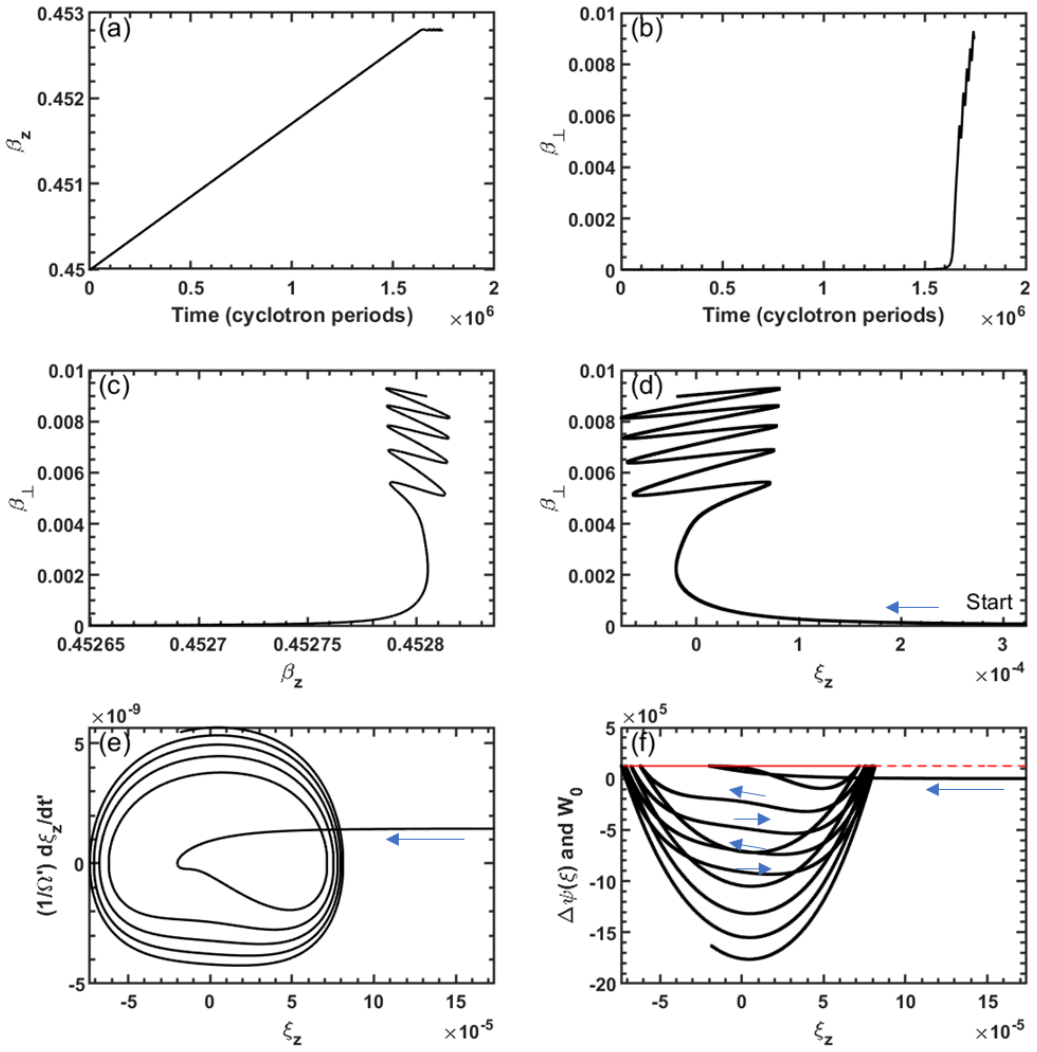

Figure 2. Same as Fig. (1) except with E_W = 22 V/m. This gives $\kappa' = 1.38 \times 10^{-7}$ but same $\frac{\zeta E_0}{cB_0} = 1.458 \times 10^{-9}$. Panels (e) and (f) show a zoomed-in view around ξ_z=0.

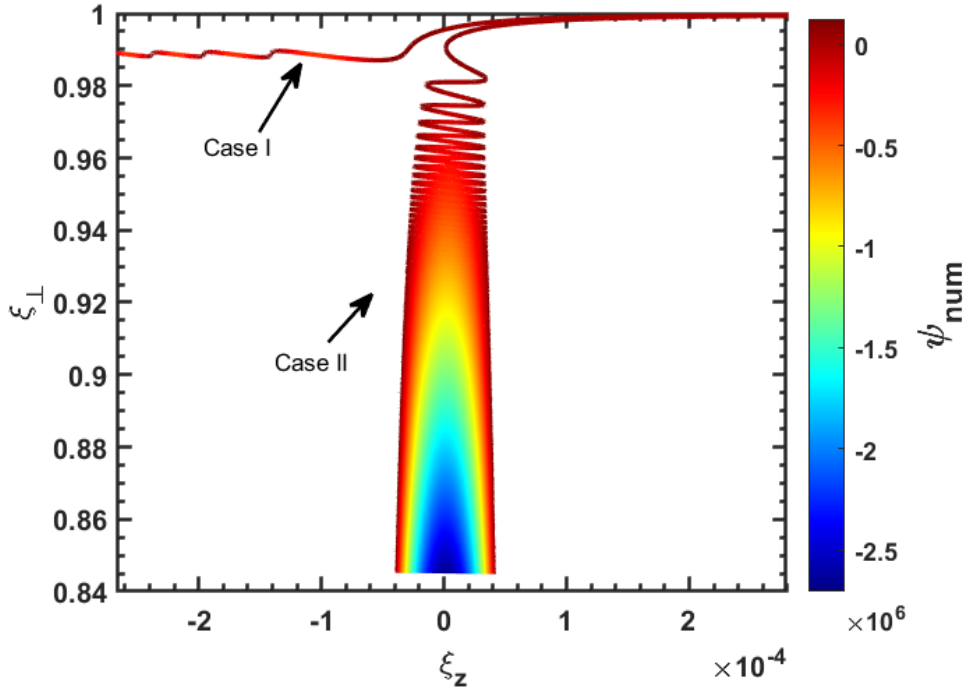

Figure 3. Pseudo-potential Δψ mapped along the electron trajectory in the ($\xi_z, \xi_\perp$) plane.

Since the pseudo-potential Δψ(ξ) is a function of both β_z and $\beta_\perp$, we traced Δψ along the particle trajectory in the ($\xi_z, \xi_\perp$) phase space. This approach highlights the underlying structure of the pseudo-potential and enables clearer physical interpretation. As shown in Fig. 3, which compares the two scenarios described in Case I and Case II. It can be seen that when the electron becomes trapped under the resonant condition, it slips into a "deep potential valley" that extends further along the $\xi_\perp$ direction. In contrast, if the electron passes through the resonant region without being trapped, it continues on a "highway"-like trajectory without further obstruction.

To determine the critical boundary of the trapping region, we refer to Eq. $(44)$and Eq.(50). Assuming the initial perpendicular velocity is approximately zero ($\beta_{\perp 0} = 0$), then s =0. Under this condition, the dynamics are governed solely by two coefficients: κ′ and $\frac{\varsigma E_0}{cB_0}$. As shown in Fig. 4, the trapping region is indicated in yellow, while the blue region corresponds to the passing regime. Case I and Case II are marked with star symbols in the figure, located in the passing and trapping regions, respectively. For special case as given in Fig.1, where $\frac{\varsigma E_0}{cB_0} = 1.458 \times 10^{-9}$, the critical threshold is $\kappa_c' = 1.367 \times 10^{-7}$, and $\frac{E_{\perp c}}{E_0} = \frac{\kappa_c' \gamma_T c B_0}{n E_0} \approx 102$. Consequently, effective electron trapping in the electromagnetic wave requires the LCP electric field intensity to exceed the background static electric field by a factor of more than 102 in typical tokamak plasma with frequencies near the upper-hybrid mode, which is agree with the result in "Constraining Electron Energy in static electric Field via the Anomalous Doppler Resonant with External Electromagnetic Waves".

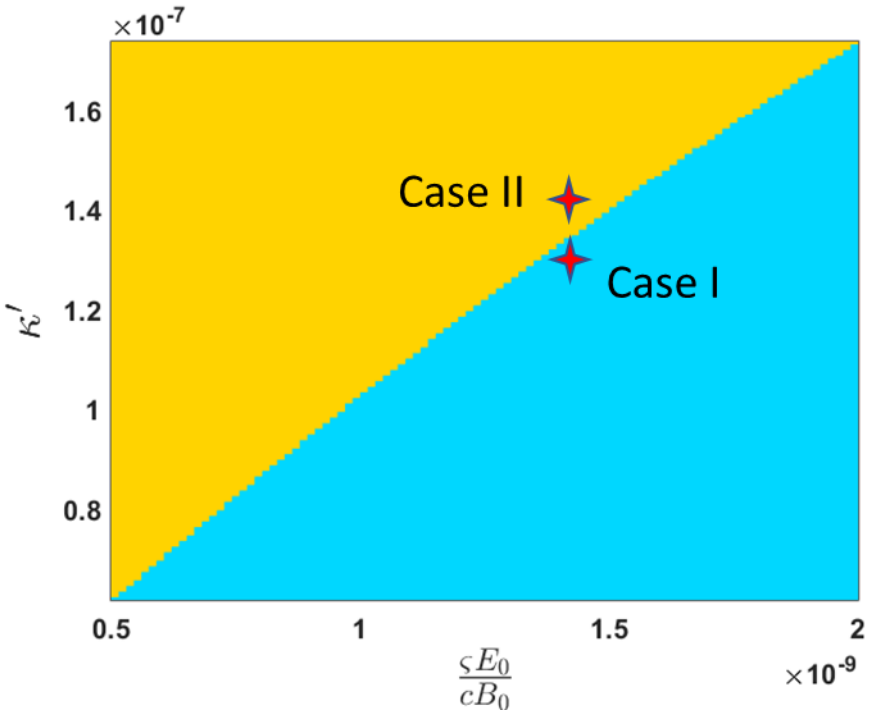

Figure 4. Parameter space of ($\frac{\varsigma E_0}{cB_0}$, κ') showing electron trapping (yellow) and passing (blue) regimes.

3.2 Trapping in normal doppler resonance (g = -1)

According to the angular momentum conservation model[27], resonance with electrons under normal Doppler resonant conditions requires that the plane electromagnetic wave possess a right-hand circularly polarized (RCP) component. To illustrate the trapping effect under the normal Doppler resonance, we consider the case where the uniform static electric field E_0 is aligned with the uniform background magnetic field B_0. A plane right-hand circularly polarized (RCP) electromagnetic wave propagates along B_0. Since the electron is accelerated in the negative B_0 direction, once resonance with the electromagnetic wave is established, the wave transfers momentum to the electron in the opposite direction of its motion. This counteracts the acceleration, thereby enabling electron trapping under resonant conditions.

To establish parameters consistent with observations from the Magnetospheric Multiscale[11] (MMS) mission, we consider Time Domain Structures (TDS) propagating at a velocity of $V_{TDS}/c\sim$ -0.0333 antiparallel to the local quasistatic magnetic field. Within the TDS, the electric field exhibits an amplitude of $E_0\sim$100 mV/m, with one half aligned parallel and the other half antiparallel to the ambient magnetic field. The background magnetic field intensity is $B_0\sim$64 nT, and the electron density is $n_e\sim$0.15 cm. In the following analysis, we examine the case in which a whistler-mode wave propagates along the magnetic field such that the corresponding normal Doppler resonance velocity coincides with V_{TDS}, so the electron also be possibility trapped in the TDS structure. Here we consider the initial electron velocity $\beta_{z0} = 0.2$ and $\beta_{\perp 0} = 0$, furthermore suppose the electron always stays in the TDS with static electric field E_0 parallel to the background magnetic field. The cold plasma dispersion relation gives that an electromagnetic wave with ω/Ω = −0.845, refractive index n = 5.4655 and have an NDE

resonant speed identical to that of the TDS.

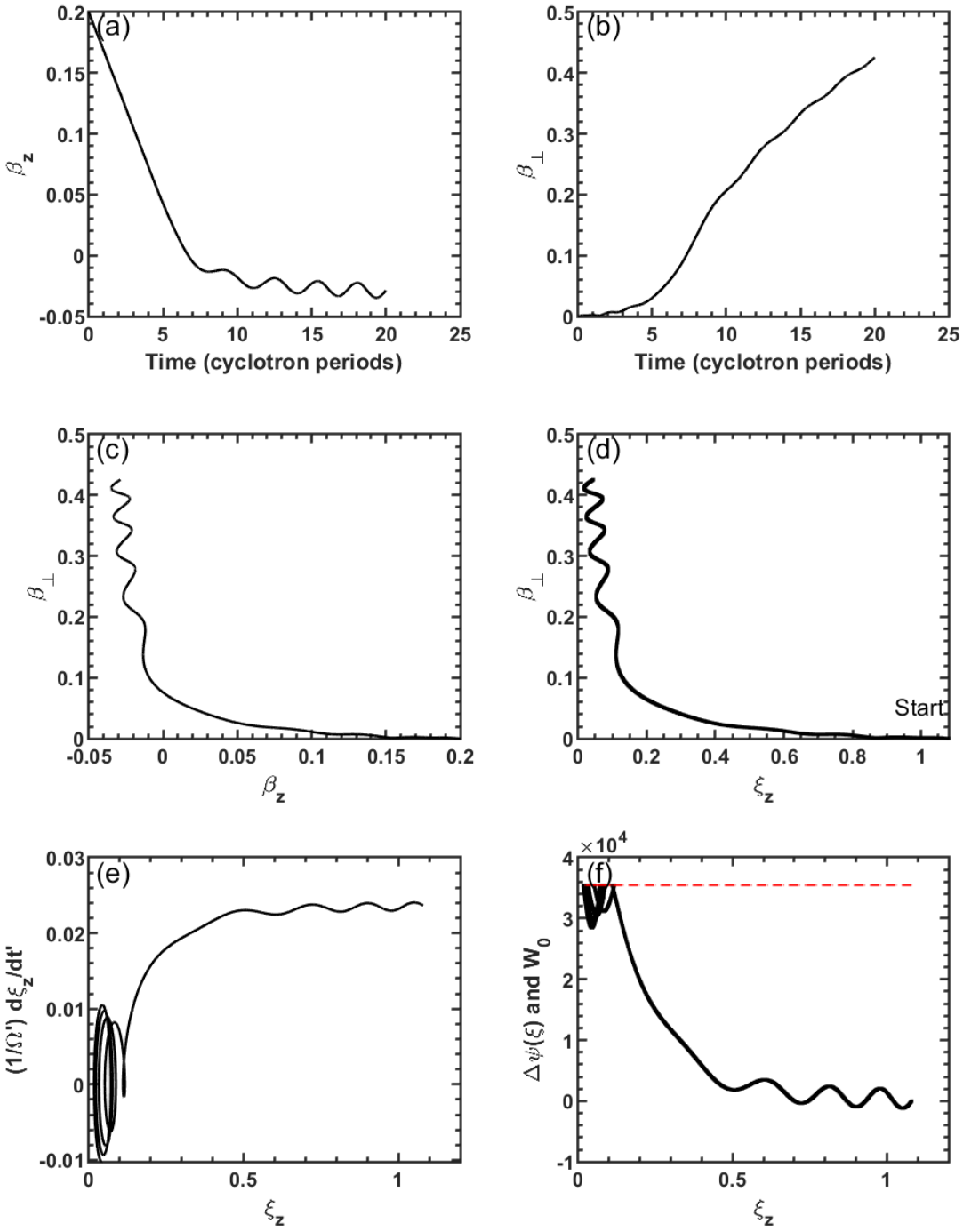

Figure 5. Same as Fig. (1) but input parameters are E0 = 100 mV/m, Ew = 0.3 V/m, B0 = 64 nT, ω/Ω = -0.845, g = -1, initial β_z= 0.2 and $\beta_\perp$=0, ϕ_0= 0, n = 5.4655. This give κ′ ≈8.2540×10^{-2},γ_T=1.0172, α=-4.5411,γ_0=1.0206 and γ′ = 1.0002 , $\frac{\varsigma E_0}{cB_0} = 0.0237$

The numerical results are shown in Fig. 5, the electron is accelerated in the opposite direction as shown in Fig.5 (a) and get trapped at $\beta_z \sim -0.03$. As trapping starts, the $\beta_\perp$ immediately increase afterward as shown in Fig. 5(b). The phase $(\beta_z, \beta_\perp)$ is shown in Fig. 5(c). The phase $(\xi_z, \beta_\perp)$ is shown in Fig. 5(d), Resonance occurs at $\xi_z = 0$, where $\beta_\perp$ exhibits a pronounced increase. The phase trajectory of

$(\xi_z, \frac{1}{\Omega'}\frac{d\xi_z}{dt'})$ is shown in Fig.5 (e), and the pseudo-potential $\Delta\psi(\xi)$ is shown in Fig.5 (f). Both exhibit the same structure as in Fig. 2.

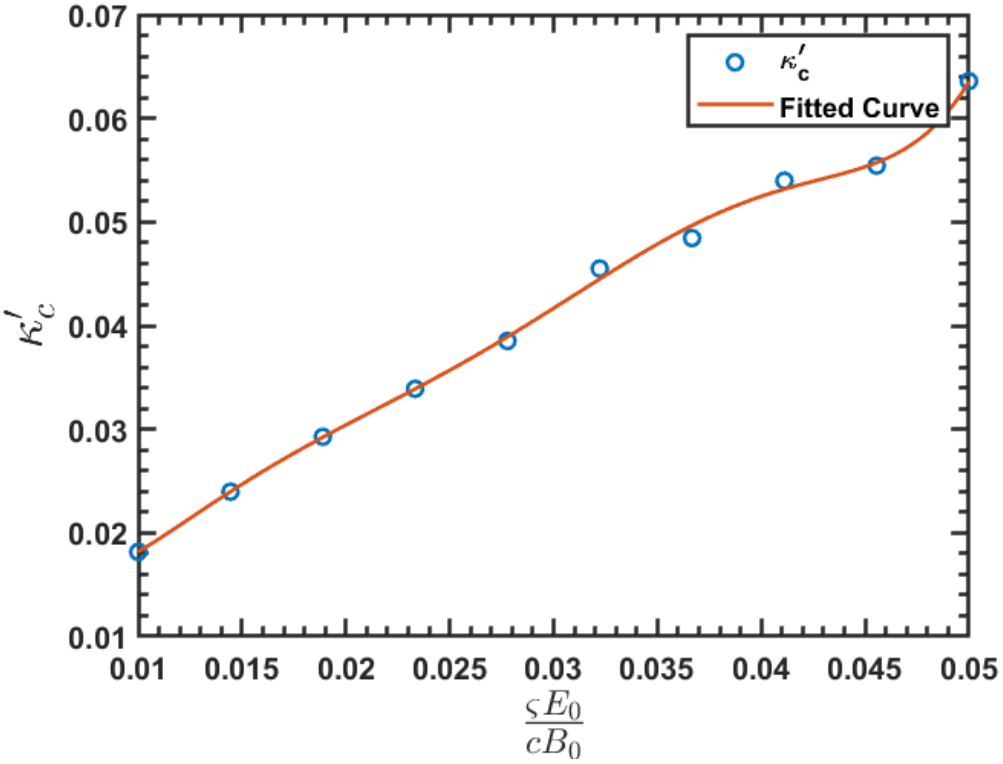

Figure 6. Critical magnetic field intensity of an E.M wave required to trap electrons under normal Doppler resonance.

Fig. 6 illustrates the critical ratio for trapping under the normal Doppler effect. In the case shown in Fig. 5, the magnetic field ratio of E.M wave is $\kappa' = 8.25 \times 10^{-2}$ at $\frac{\varsigma E_0}{cB_0} = 0.0237$, while the critical ratio is $\kappa_c' = 3.3 \times 10^{-2}$. Since $\kappa' > \kappa_c'$, the wave amplitude exceeds the threshold required for trapping, allowing electrons to be captured by the wave, as observed in Fig. 5.

IV. Benchmark with quantum theory

One characteristic worth pointing out is that when the electron is trapped in the electromagnetic wave, the energy transfer from the static electric field to the gyrokinetic energy is governed by quantum theory (QE theory) [28]

$$\eta_p = \frac{n|\Omega|/\gamma_c}{k \cdot v} \tag{61}$$

Here γ_c refers to the Lorentz factor during the resonance. For anomalous Doppler resonance, n = 1 and $k \cdot v = \omega + |\Omega|/\gamma_c$, η_p can be written as

$$\eta_p = \frac{1}{1 + |\omega/\Omega|\gamma_c} \tag{62}$$

For Case II, $\frac{\omega}{\Omega} = -1.1$ and $\gamma_c = 1.1215$ we have η_p =0.448. To numerically calculate the energy transfer ratio, we evaluate the work done by the static electric field during resonance:

$$W_E = \int_0^t E_0 q v_z dt - \int_0^{t_c} E_0 q v_z dt \tag{63}$$

Here τ_c refers to the beginning of trapping time. The increase of perpendicular energy is given by

$$W_\perp = \frac{1}{2} m v_\perp^2 \tag{64}$$

Finally, the energy transfer ratio is calculated as $\eta_p = W_\perp / W_E$.

The η_p values obtained from the two methods are illustrated in Fig. 7. As the electron is trapped by electromagnetic wave, the energy transfer ratio from the numerical results tends to approach the theoretical prediction, and this ratio is independent of the wave's intensity. The agreement between the numerical and theoretical results confirms both the accuracy of the simulation and the consistency between quantum theory and classical dynamics.

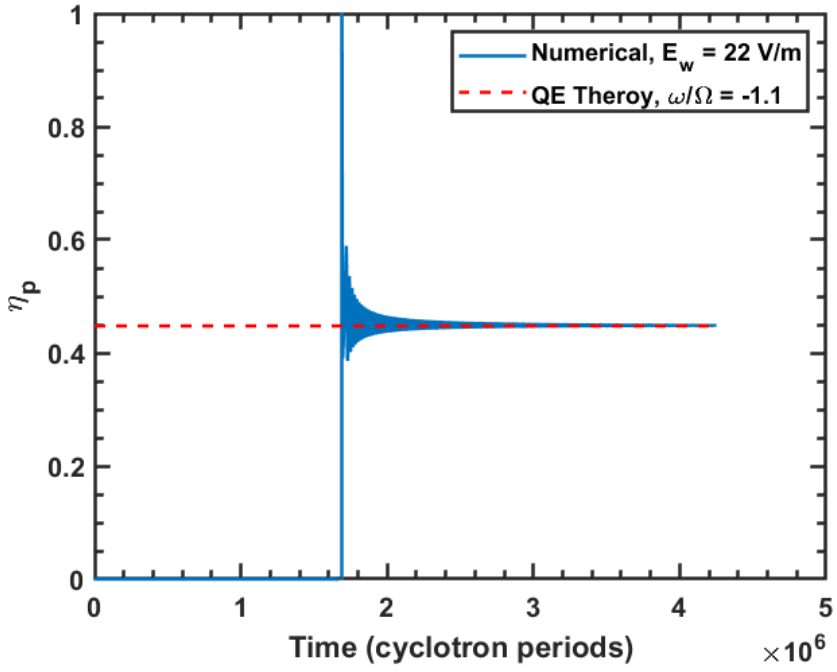

Figure 7.Energy transfer ratio from the static electric field to the gyrokinetic energy. The parameters used here are the same as in Figure 2 (QE theory means theory based on quantum equation).

V. Discussion

This trapping effect can also be qualitatively understood through the conservation of angular momentum and linear momentum. We can draw an analogy by treating the cyclotron electron as a system that contains both internal and kinetic energy, where the internal energy refers to gyrokinetic

energy and kinetic energy refers to its translational motion along the magnetic field. When this system is stimulated by an external E.M wave, it undergoes stimulated emission (absorption), radiating (absorbing) E.M wave identical to the external one.

For anomalous doppler resonance, Since the emitted E.M wave propagates in the same direction as the electron, conservation of linear momentum requires the electron to lose some of its parallel momentum. At the same time, because the electron possesses right-hand circularly rotation (associated with positive angular momentum), while the emitted wave has left-hand circularly polarization (associated with negative angular momentum, conservation of total angular momentum requires the electron to gain angular momentum after emission. As a result, the electron loses kinetic energy and gains gyrokinetic energy. However, a static electric field continues to replenish the lost kinetic energy. When the rate of energy loss to the E.M wave balances the energy input from the electric field, the electron's parallel velocity ceases to increase, and the electron becomes trapped in the electromagnetic wave. This manifests as a continuous transfer of energy from the static electric field to the gyrokinetic energy of the system.

This explanation could also apply to the normal Doppler resonance trapping effect. When the E.M wave propagates in the reverse direction of the electron, resonance and absorption cause the electron’s gyrokinetic energy to increase through angular momentum conservation, since the E.M wave carries right-hand circular polarization matching the electron’s cyclotron rotation. Simultaneously, the electron’s parallel velocity decreases as it absorbs the photon momentum in the opposite direction. Once the momentum loss balances the gain from the static electric field, the electron’s parallel velocity saturates and becomes trapped in the resonant condition, while its gyrokinetic energy continues to increase.

Beyond the theoretical significance, these results have two main areas of potential application:

(a)Runaway Electron Control and Plasma Heating in Tokamaks

The redistribution of electron energy between parallel motion and gyrokinetic energy suggests a possible route for mitigating runaway electrons. Tailored wave injections (e.g., whistler-mode or electron cyclotron waves) could induce resonant trapping, helping to suppress runaway electrons. At the same time, the continuous energy transfer from static electric fields to gyrokinetic energy may provide a novel pathway for plasma heating, complementing established methods such as electron cyclotron resonance heating (ECRH).

(b)Space Plasma Dynamics

The trapping mechanism closely parallels processes observed in planetary magnetospheres, such as electron interactions with whistler-mode chorus waves or time-domain structures. The pseudo-potential approach developed here could therefore offer new insights into particle acceleration, precipitation, and radiation belt dynamics in Earth and planetary space environments.

These focused applications highlight the relevance of resonant trapping to both controlled fusion research and space plasma physics, suggesting directions for future experimental validation and theoretical development.

VI. Summary

In conclusion, trapping under both normal and anomalous Doppler resonances is analyzed via the pseudo-potential approach. The parallel velocity oscillates within a potential well, while the perpendicular velocity grows continuously. Critical trapping energy is obtained numerically, with energy conservation ratios from simulations and quantum theory showing strong agreement. The mechanism is explained through angular and linear momentum conservation, and potential applications and phenomena are discussed.

Appendix:

a. Prove the relationship between resonant condition and ξ

The parameter ξ characterizes the frequency mismatch relative to the resonance condition given by

$$\omega = \boldsymbol{k} \cdot \boldsymbol{v} + g\frac{\Omega}{\gamma} \tag{65}$$

This relationship can be derived as follows: Starting from the definition of ς as shown in Eq.(43), we have:

$$\varsigma\beta_z' = \frac{\omega}{\Omega}\frac{n}{\gamma_T}\gamma'\beta_z' \tag{66}$$

Since $\{\gamma\beta, \gamma\}$ are four-vector, we have

$$\gamma'\beta_z' = \gamma_T(\gamma\beta_z - \beta_T\gamma) = \gamma_T\gamma\left(\beta_z - \tfrac{1}{n}\right) \tag{67}$$

Substituting Eq. (67) and Eq. (66) into Eq. (13) gives

$$\xi_z = 1 + g\frac{\omega}{\Omega}\frac{n}{\gamma_T}\gamma_T\gamma\left(\beta_z - \frac{1}{n}\right) = g\frac{g\frac{\Omega}{\gamma} + k\cdot v - \omega}{\frac{\Omega}{\gamma}} \tag{68}$$

Here $g\frac{\Omega}{\gamma} + k\cdot v - \omega = 0$ represents the resonant condition.

References

[1] Golovanivsky K S 1982 The Gyrac - a Proposed Gyro-Resonant Accelerator of Electrons *Ieee T Plasma Sci* **10** 120-9

[2] Gal O 1989 GYRAC: a compact, cyclic electron accelerator *Ieee T Plasma Sci* **17** 622-9
[3] Shprits Y Y, Runov A and Ni B 2013 Gyro-resonant scattering of radiation belt electrons during the solar minimum by fast magnetosonic waves *Journal of Geophysical Research: Space Physics* **118** 648-52
[4] Pukhov A, Sheng Z M and Meyer-ter-Vehn J 1999 Particle acceleration in relativistic laser channels *Physics of Plasmas* **6** 2847-54
[5] Bai M, Lee S, Glenn J, Huang H, Ratner L, Roser T, Syphers M and Van Asselt W 1997 Experimental test of coherent betatron resonance excitations *Physical Review E* **56** 6002
[6] Baartman R 1995 Betatron resonances with space charge *Proceedings of Space Charge Physics in High Intensity Hadron Rings (Shelter Island, New York, USA, 1998)*
[7] Tajima T and Dawson J M 1979 Laser Electron-Accelerator *Physical Review Letters* **43** 267-70
[8] Yu W, Yu M, Ma J, Sheng Z, Zhang J, Daido H, Liu S, Xu Z and Li R 2000 Ponderomotive acceleration of electrons at the focus of high intensity lasers *Physical Review E* **61** R2220
[9] Gary S P, Montgomery D and Swift D W 1968 Particle Acceleration by Electrostatic Waves with Spatially Varying Phase Velocities *Journal of Geophysical Research* **73** 7524-+
[10] Sheena Z, Ruschin S, Gover A and Kleinman H 1990 High-Efficiency Nonadiabatic Trapping of Electrons in the Ponderomotive Potential Wells of Laser Beats *Ieee J Quantum Elect* **26** 203-6
[11] Mozer F, Agapitov O, Giles B and Vasko I 2018 Direct observation of electron distributions inside millisecond duration electron holes *Physical Review Letters* **121** 135102
[12] Grach V S, Artemyev A V, Demekhov A G, Zhang X J, Bortnik J, Angelopoulos V, Nakamura R, Tsai E, Wilkins C and Roberts O W 2022 Relativistic electron precipitation by EMIC waves: Importance of nonlinear resonant effects *Geophysical Research Letters* **49** e2022GL099994
[13] Millan R and Baker D 2012 Acceleration of particles to high energies in Earth's radiation belts *Space Science Reviews* **173** 103-31
[14] Bellan P M 2013 Pitch angle scattering of an energetic magnetized particle by a circularly polarized electromagnetic wave *Physics of Plasmas* **20**
[15] Bourdier A and Gond S 2000 Dynamics of a charged particle in a circularly polarized traveling electromagnetic wave *Physical Review E* **62** 4189-206
[16] Liu H, He X, Chen S and Zhang W 2004 Particle acceleration through the resonance of high magnetic field and high frequency electromagnetic wave *arXiv preprint physics/0411183*
[17] Nusinovich G S, Korol M and Jerby E 1999 Theory of the anomalous Doppler cyclotron-resonance-maser amplifier with tapered parameters *Physical Review E* **59** 2311
[18] Nusinovich G S, Latham P and Dumbrajs O 1995 Theory of relativistic cyclotron masers *Physical Review E* **52** 998
[19] Qian B L 1999 An exact solution of the relativistic equation of motion of a charged particle driven by a circularly polarized electromagnetic wave and a constant magnetic field *Ieee T Plasma Sci* **27** 1578-81
[20] Qian B L 2000 Relativistic motion of a charged particle in a superposition of circularly polarized plane electromagnetic waves and a uniform magnetic field *Physics of Plasmas* **7** 537-43
[21] Roberts C S and Buchsbaum S 1964 Motion of a charged particle in a constant magnetic field and a transverse electromagnetic wave propagating along the field *Physical Review* **135** A381
[22] Weyssow B 1990 Motion of a single charged particle in electromagnetic fields with cyclotron resonances *Journal of plasma physics* **43** 119-39
[23] Mozer F, Agapitov O, Krasnoselskikh V, Lejosne S, Reeves G and Roth I 2014 Direct observation of radiation-belt electron acceleration from electron-volt energies to megavolts by nonlinear whistlers *Physical review letters* **113** 035001
[24] Artemyev A, Agapitov O, Mozer F and Krasnoselskikh V 2014 Thermal electron acceleration by localized bursts of electric field in the radiation belts *Geophysical Research Letters* **41** 5734-9

[25] Liu C, Hirvijoki E, Fu G-Y, Brennan D P, Bhattacharjee A and Paz-Soldan C 2018 Role of kinetic instability in runaway-electron avalanches and elevated critical electric fields *Physical Review Letters* **120** 265001
[26] Xie Z-K, Zong Q-G, Yue C, Zhou X-Z, Liu Z-Y, He J-S, Hao Y-X, Ng C-S, Zhang H and Yao S-T 2024 Electron scale coherent structure as micro accelerator in the Earth's magnetosheath *Nature Communications* **15** 886
[27] Xu X, Xie J, Liu J and Liu W 2025 Analysis of the Anomalous Doppler Effect from Quantum Theory to Classical Dynamics Simulations *Chinese Physics B*
[28] Nezlin M V 1976 Negative-energy waves and the anomalous Doppler effect *Soviet Physics Uspekhi* **19** 946